Indian Journal of Chemical Technology
Vol. 23, July 2016, pp. 271-278

Corrosion behaviour of electrodeposited Zn–Co–Fe alloy

Mortaga Abou-Krisha*[,1,2], Fawzi Assaf[1], Omer Alduaij[2], Abdelrahman Alshammari[2] & Fatma El-Sheref[1]

[1]Faculty of Science, Chemistry Department, South Valley University, Qena, 83523, Egypt.

[2]College of Science, Chemistry Department, Al Imam Mohammad Ibn Saud Islamic University (IMSIU), Riyadh 11623, KSA.

E-mail: m_abou_krisha@yahoo.com

Received 2 May 2014; accepted 16 October 2014

The anodic dissolution and passivation of Zn–Co–Fe alloy film; deposited galvanostatically on a steel rod from a sulfate bath, has been studied in 0.5 M NaOH. The study is carried out using electrochemical methods such as, galvanostatic measurements for electrodeposition, cyclic voltammetry (CV) for the anodic and cathodic behaviour of alloy to study the potential ranges at which the oxidation and reduction processes occur. Anodic linear sweep voltammetry (ALSV) technique is used for the phase structure determination. The values of parameters such as scan rate and the influence of concentration and temperature of NaOH solution have been varied to study their effect on the electrodeposited Zn–Co–Fe alloy. X-ray Diffraction (XRD) show that Zn–Co–Fe alloy coatings consist of a zinc solid solution and iron–cobalt intermetallic phase (FeCo). It is found that the anodic excursion exhibited two anodic dissolution peaks A_1 and A_2. The first anodic peak A_1 related to the dissolution of Zn from pure zinc phase and the second A_2 to the complex dissolution of the elements iron and cobalt from their homogeneous FeCo phase. Increasing the scan rate enhance the height of the anodic peak and shifts potentials to nobler values, which may be due to the selective dissolution of zinc increases. Increasing NaOH concentration and temperature, accelerates the diffusion rate of the diffusing species to or from the anode surface, results in increasing the height of the anodic peak and shift their potentials towards more negative values.

Keywords: Electrodeposited Zn–Co–Fe alloy, Corrosion behaviour, Cyclic voltammetry

It has been shown that zinc alloys can provide improved the corrosion resistance for ferrous substrates mainly in the automobile industry compared to pure zinc in which the corrosion resistance is not satisfactory and unacceptable under sever atmospheric conditions[1]. Also, Zn alloys used as a substitute for toxic and high-cost cadmium coatings[2,3]. The most common zinc alloys are Zn–Co, Zn–Fe and Zn–Ni[2,4]. The electrodeposition of Zn–Co alloys is interesting because these alloys exhibit a significantly higher corrosion resistance and better surface morphology than pure zinc coatings[5]. Coatings with high Co content are nobler than steel, provide a barrier type of protection[6,7]. On the other hand, the electrodeposited Zn–Fe alloy coatings possess many excellent properties, such as high corrosion resistance due to the nature of the Zn–Fe phase, excellent paintability and good welding properties of Zn–Fe phase in comparison to the pure zinc[8]. Zn–Fe alloys exist in various phases, and also their structure and morphology[9] determines the corrosion resistance of a deposit. Many research groups have reported the preparation of these alloys with high or low iron content, respectively[10,11]. The codeposition of Fe into the binary Zn-Co alloy or Co into the binary Zn–Fe alloy leads to improve the characteristics and performance of the produced ternary Zn–Co–Fe alloy. Recently there is a growing interest on the electrodeposited Zn–Co–Fe alloy because of their superior protective properties[12-14]. Conceicao *et. al.*[14] were studied the corrosion behaviour of electrodeposits of zinc and zinc alloys by means of electrochemical tests in an aerated solution of 3.5% (0.6 M) NaCl at *p*H 8.2. They concluded that the Fe presence in the alloy results in a good adhesion to the substrate and allows application of these materials at high temperatures.

Many metals and alloys suffer from pitting corrosion in different environments; among these metals are Zn and its alloys. Therefore the present paper aims to study the anodic dissolution process of Zn–Co–Fe alloy, electrodeposited galvanostatically on a steel rod, in 0.5 M NaOH solution. Also study the influence of varying scan rate; temperature and concentration of NaOH solution on electrodeposited Zn–Co–Fe alloy.

Experimental Section

Pure Zn, Fe and Co; Zn–Co, Zn–Fe, Fe–Co and Zn–Co–Fe alloys were electrodeposited galvanostatically on steel rod from a sulfate bath of the following composition 0.2 M $ZnSO_4$, 0.2 M $CoSO_4$, 0.2 M $FeSO_4$, 0.2 M Na_2SO_4, 0.2 M H_3BO_3 and 0.01 M H_2SO_4. The electrolytes used for the electrodeposition of different deposits were freshly prepared using Analar grade chemicals without further purification and dissolved in appropriate amounts of double distilled water. All experiments have been carried out in duplicate; the measurements have shown good reproducibility. The *p*H of the plating bath was measured at 30.0°C ± 1°C and was found to be 2.5 ± 0.02. The deposits were obtained on a pure steel rod, which prepared in a Teflon mount with a geometrical area 0.196 cm^2 for electrochemical studies. For morphological properties (SEM) and contents determination of the electrodeposited alloy study, 1.0 cm of width and length of the stainless steel sheet cathode was used. Electrodeposition of alloy on copper sheet was used for EDX and XRD analysis to prevent the difficulties due to that the deposit contains Fe. Before each experiment the surface of the steel rod electrode was hand polish with emery paper (up to 1500) then immersed in ethyl alcohol and rinsed with doubly distilled water and then dried. After surface preparations, the steel immediately placed in the plating bath. The electrolytic cell was used in the present work as detailed in literature[15]. Before each run, the cell was cleaned with chromic/sulfuric mixture, washed with first and second distilled water and filled with 50 cm^3 of the electrolyte of temperature 30.0°C. The counter electrode was a platinum electrode and the reference electrode was standard calomel electrode (SCE). Cyclic voltammetry and anodic linear sweep voltammetry experiments of Zn–Co–Fe alloy, electrodeposited galvanostatically on steel rod were studied in 0.5 M NaOH solution with *p*H=12 at 30.0°C using potential range from -1500 mV in the positive direction, and reversed at 500 mV in the negative direction and at scan rate of 50 mV s^{-1}.

Electrochemical experiments were carried out in a conventional three electrode cell using an EG&G potentiostat/galvanostat model 273A controlled by a PC containing corrosion analysis software model 352. The surface morphology of the coatings was characterized by (SEM) model JSM-5500 LV (JEOL). The qualitative and semiquantitative chemical analysis of the Zn–Co–Fe alloy was determined via (EDXRF) model JEOL JSX 3222. The phase compositions of Zn–Co–Fe alloy deposit were determined by (XRD) model Brucker Axs-D8 Advance with CuK-α radiation (λ= 1.5406 A^o and 40 mA).

Results and Discussion

Galvanostatic measurements

Figure 1 shows the potential–time dependence for the deposition of pure Zn, Co and Fe; Zn–Co and Zn–Fe for binary alloys and Zn–Co–Fe for ternary alloy on steel rod at 10 mA cm^{-2} for 10 min. Contents % of the various coatings were observed in Table 1. It is clear that the deposition of the pure Co and Fe needs low overpotential to create the initial nucleus and the deposit grows at low potentials. However, the deposition of pure Zn takes place with higher nucleation overpotential and grows at high potential. The Zn–Co [pure Zn and γ-phase (Co5Zn21)[3]] and Zn–Fe [pure zinc and $Zn_{21}Fe_5$ phase] alloys are codeposited at moderate overpotential values lying between Zn overpotential; and Co and Fe overpotentials. This is because the deposition of Co or Fe is strongly inhibited by the presence of Zn^{+2}, while the deposition of Zn is induced by the presence of Co^{+2} and/or Fe^{+2}. On the other hand, Zn–Co–Fe alloy

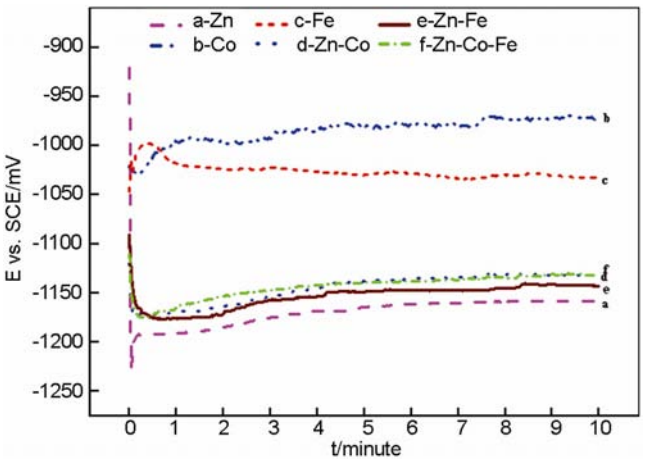

Fig. 1 — E-t curves for deposition of various coatings on steel cathode.

Table 1 — Contents % of the various coatings on the stainless steel sheet substrate.

	Deposit					
Parameter	Zn	Co	Fe	Zn-Fe	Zn-Co	Zn-Co-Fe
Zn content %	100	0	0	73.8	97.3	65.8
Co content %	0	100	0	0	2.7	8.9
Fe content %	0	0	100	26.2	0	25.3

is codeposited at nobler overpotential than Zn-Co and Zn-Fe alloys. The potential of Zn–Co–Fe alloy is more negative than that of pure Fe and Co under the same conditions. Basically, corrosion potential of Zn–Co–Fe alloy is negatively compared to pure Fe and Co and nobler than pure Zn, Zn–Fe and Zn–Co binary alloy. Moreover, for E-t curves the potential starts with a maximum value, then decrease gradually with time. The initial decreasing potential corresponding to the charging of the double layer, followed by a rising of potential due to either the growth of a new phase and/or to an increase of the number of nuclei[16,17]. Finally, the potential falls, corresponding to linear diffusion. These findings suggest that the electrodeposition process is diffusion controlled by a typical nucleation mechanism[18].

Figure 2a shows the XRD pattern of the electrodeposited Zn–Co–Fe alloy on copper sheet revealing the presence of pure Zn and Fe/FeCo phase in the deposited film. It is obvious from this figure the overlapping of FeCo and Fe phases[19]. EDXF analysis was carried out to investigate the metal percentage of the deposit. Distinct peaks for metals were observed by EDXF analysis of the deposit which confirms the formation of Zn–Co–Fe alloy on copper sheet; their compositions are quantified in Fig. 2b. It can be observed from the peaks the presence of sulfur peak due to the reduction of sulfate group to sulfur[20]. Also, the presence of copper peak due to the electrodeposition of Zn–Co–Fe alloy was on copper sheet.

The grain size of the deposited alloys was calculated using Scherrer equation (1).

$$D = \frac{K\lambda}{\beta \cos\theta} \quad \ldots (1)$$

where K is taken as 1, λ the wave length of X-ray used and β the full width of the half maximum of the peak. The grain size was calculated around the most intense peak. The calculated grain size for Zn-Co-Fe film is small and existence in the nano size range 32 nm.

The surface morphology of Zn–Co–Fe alloy deposits from the plating bath is shown in Fig. 3, which indicates the complete coating, compact and homogeneous deposits on the substrate surface.

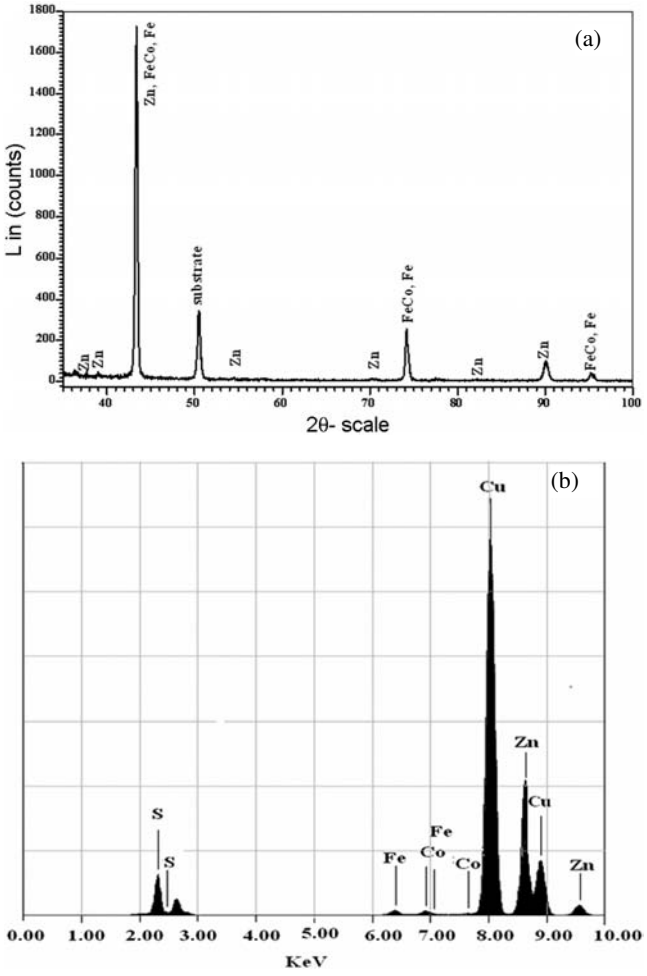

Fig. 2 — A- XRD patterns and B- EDX peaks for Zn-Co-Fe alloy, electrodeposited galvanostatically on a copper substrate

Cyclic voltammograms measurements

Cyclic voltammograms of pure Zn, Fe, Co; Zn–Fe, Zn–Co, Fe–Co binary alloys and Zn–Co–Fe ternary alloy

Figures 4a-b show the cyclic voltammetric behaviour of the electrodeposited pure Zn, Fe and Co; Zn–Fe, Zn–Co, Fe–Co binary alloys and Zn–Co–Fe ternary alloy obtained on steel rod substrate in 0.5 M

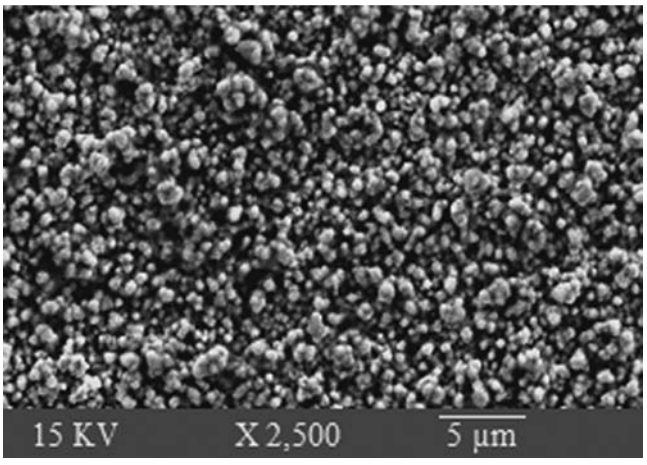

Fig. 3 — SEM photograph for Zn-Co-Fe alloy, electrodeposited galvanostatically on a stainless steel substrate.

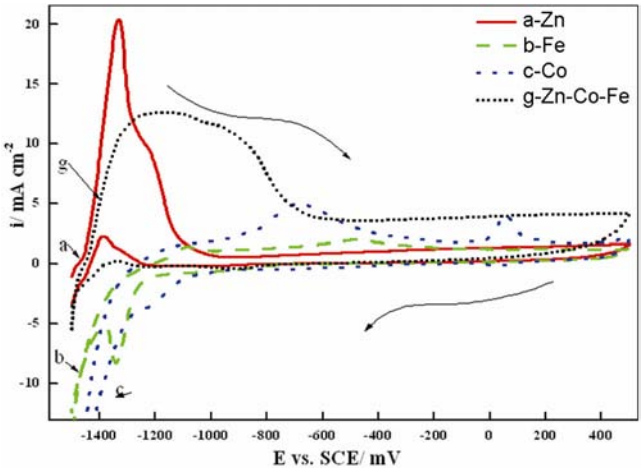

(a)

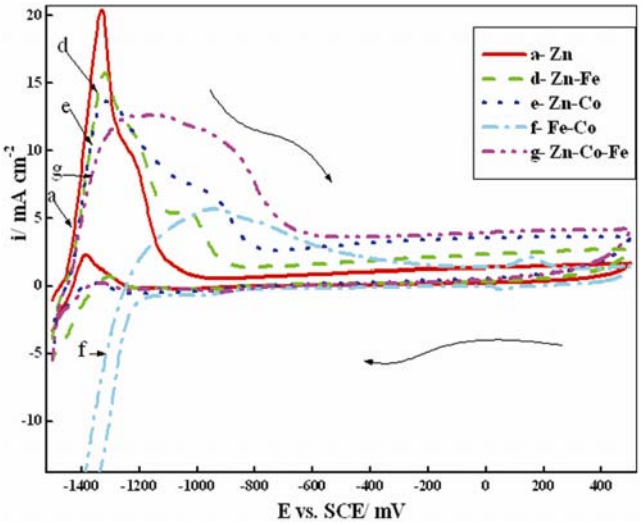

(b)

Fig. 4a & 4b — i-E curves (cyclic voltammograms) of Zn, Co, Fe, Zn-Co, Zn-Fe, Fe-Co and Zn-Co-Fe deposits, in 0.50 M NaOH solution between E_c= -1500 mV and E_a= 500 mV at scan rate 50 mV s^{-1} and 30.0°C.

NaOH at 30.0°C. The potential scan was started in the positive direction from -1500 mV and reversed at 500 mV in the negative direction with a scan rate 50 mV s^{-1}.

Curve (a) represents the cyclic voltammogram of the electrodeposited zinc deposit. The anodic scan shows two anodic dissolution peaks at potentials -1330 mV and -1220 mV, respectively. Zinc dissolves in the alkali to give two peaks, the first peak corresponds to Zn to $Zn(OH)_2$ and the second type of $Zn(OH)_2$ to ZnO[21,22], till the dissolution reaches to a passive state. The cathodic scan shows a clear anodic peak this may be due to a reactivation of the electrodissolution process in the potential range from -1300 mV to -1425 mV.

Two anodic peaks appear in the positive scan of iron (curve b). The first peak is due to the dissolution of iron to Fe^{+2} (-1088 mV) and the second represents Fe^{+2} to Fe^{+3} (-500 mV). The deposition of iron shows two reduction peaks, the reduction of iron complexes represents the first deposition peak at potential -905 mV, beyond -1340 mV bulk deposition of Fe occurs simultaneously to H_2 evolution reaction (HER).

From the anodic scan of cobalt (curve c), the two peaks are observed at -678 mV and -61 mV[23], respectively which correspond to cobalt dissolution. Two reduction peaks of cobalt are shown at potentials 0.0 mV and -1200 mV, respectively, owing to the deposition of cobalt ions to cobalt which occurs simultaneously to HER for the second cathodic peak.

Zn–Fe alloy anodic voltammogram (curve d) shows three dissolution peaks (-1320 mV, -1202 mV and -1000 mV, respectively). The first and second peaks belong to dissolution of zinc, but the third represents iron, this result of dissolution of Zn–Fe alloy differs with L. L. Barbosa *et al.*[24] in which electrodeposited Zn-Fe alloy with non cyanide bath dissolved as one metal. Two cathodic peaks at potentials -922 and -1207 mV, respectively, are observed, which attributed to the deposition of iron for the first peak and deposition of zinc and iron for the second peak. An anodic peak appears in the cathodic region at potential -1307 mV which may be due to the dissolution of zinc during the deposition process.

The positive scan for Zn–Co alloy (curve e) shows the zinc dissolution at potential -1300 mV from pure zinc phase and zinc from Zn-Co phase also at -900 mV another anodic peak appears according to the dissolution of the Co from Zn-Co phase[25]. In the cathodic region two cathodic peaks appear at potentials -1013 and -1233 mV due to the deposition of cobalt for the first cathodic peak and deposition of zinc and cobalt for the second one.

The cyclic voltammogram for Co–Fe alloy (curve f) represents two dissolution peaks in the anodic direction. A wide peak appears at potential -998 mV which belongs to the oxidation of iron and/or cobalt and the second peak at more positive potentials 139 mV to dissolution of cobalt. When the scan is reserved, two cathodic peaks are observed. A peak at more positive potential 58.2 mV this peak can be attributed to the reduction of cobalt and the second

peak at -992 mV, corresponds the deposition of cobalt and iron together.

Curve (g) shows the cyclic voltammogram recorded for dissolution and deposition of the constituents of Zn–Co–Fe alloy. The dissolution of alloy starts with zinc at potential -1300 mV. Also, there is another anodic dissolution peak at potential -970 mV, this peak has a complete homogeneity of the two components Fe and Co which behaves like one metal and dissolves simultaneously. The onset of alloy deposition relates to cobalt and iron at -922 mV and the second deposition peak at -1237 mV may be to all of the components; cobalt, iron and zinc.

From the cyclic voltammogram curves for Zn–Co, Zn–Fe and Zn–Co–Fe alloys, it is noticeable that the reduction peaks are very small except nearly the deposition potential of Zn. This phenomena may be attributed to that the cathodic deposition occurs in/from firstly; alkaline bath, secondly; the amount of deposits which dissolve during the anodic scan are very small dissolved metals finally; the anomalous codeposition especially in the alkaline media (hydroxide suppression mechanism)[1].

Effect of scan rate

The effect of increasing the potential scan rate (υ) was investigated for Zn–Co–Fe alloy which electrodeposited galvanostatically on steel rod substrate and dissolved anodically in 0.5 M NaOH at 30.0°C. Figure 5 represents the cyclic voltammogram curves of the electrodeposited Zn–Co–Fe film with various scan rates. From the anodic scan it seems that, two anodic dissolution peaks can be seen. At scan rates 25 and 50 mV s^{-1}, it's interesting to see in the cathodic scan a reactivation of the electrodissolution process in alkaline media at potential range from -1300 mV to -1425 mV that may be due to that at more negative potentials zinc prefers to be in zinc ions form.

At low scan rate (ν), oxides and hydroxides of zinc, iron and cobalt are formed in alkaline media causing a decrease in the anodic peak current density. Increasing the potential scan rate increases the height of the anodic peak current density (i_p) and shifts potentials in a more positive direction that may be due to the selective dissolution of zinc, which takes place forming zinc oxide and/or hydroxide leaving iron and cobalt as it.

Figure 6 represents the linear dependence of the peak current density of the anodic peak (i_p) on the square root of the sweep rate of the electrodeposited Zn-Co-Fe alloy. There is a relatively good linear relationship between the current densities and the square root of the scan rates ($\nu^{1/2}$). It is also found that the peak potential of the anodic peaks (E_p) values showed linear variations with the logarithmic scan rate, Fig. 7. The linear relationships indicate that the processes involved in the appearance of these peaks are diffusion-controlled processes. The relation between i_p and $\nu^{1/2}$ is described by the Randles-Sevcik equation:

$$i_p = (269{,}000)n^{3/2}AD^{1/2}C\nu^{1/2}$$

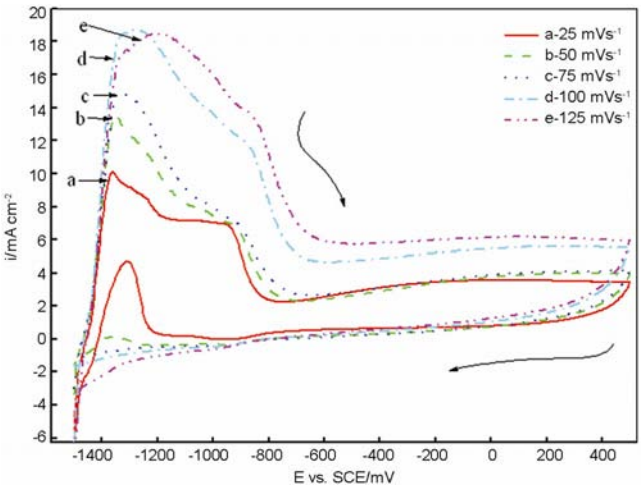

Fig. 5 — i-E curves (cyclic voltammograms) for Zn-Co-Fe alloy, electrodeposited galvanostatically on steel substrate, in 0.50 M NaOH solution between E_c= -1500 mV and E_a= 500 mV at 30.0°C, at different scan rates.

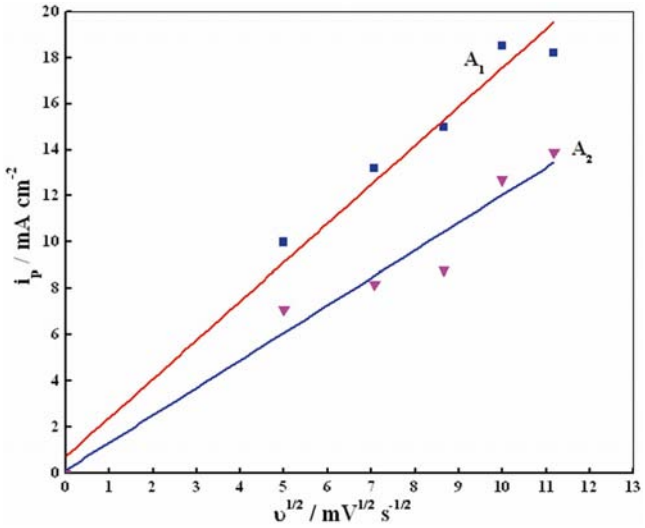

Fig. 6 — Relation between the peak current density (i_p) and the root of scan rate ($\nu^{1/2}$) for the anodic peaks A_1 and A_2 for Zn-Co-Fe alloy, electrodeposited galvanostatically on steel substrate and dissolved in 0.5 M NaOH solution at 30.0°C.

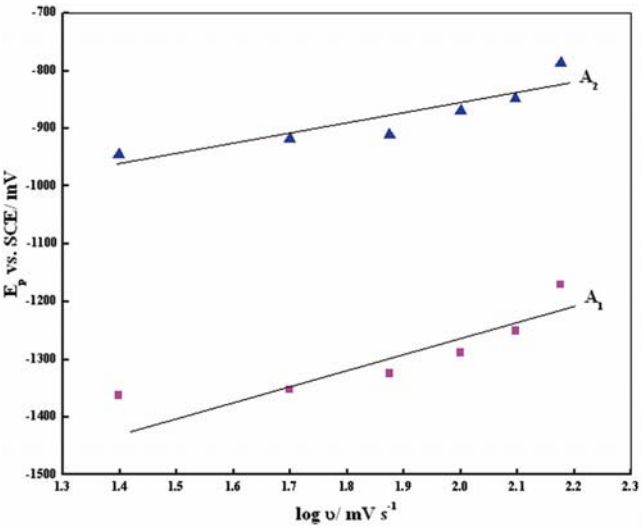

Fig. 7 — Relation between the peak potentials (E_p) and the log of scan rates (log ν) for the anodic peaks A_1 and A_2 for Zn-Co-Fe alloy, electrodeposited galvanostatically on steel substrate and dissolved in 0.5 M NaOH solution at 30.0°C.

where i_p = current maximum in amps, n = number of electrons transferred in the redox event (usually 1), A = electrode area in cm^2, F = The Faraday constant in C mol^{-1}, D = diffusion coefficient in cm^2/ s, C = concentration in mol / cm^3, v = scan rate in V/ s.

From Fig. 6, the linear correlation coefficients (r) were calculated and being equal, 0.991 for A_1 and for A_2, r = 0.981. This means that the lines in accordance with Randles equation. It is important to remember that current, i, is charge (or electrons passed) per unit time. Therefore, at faster voltage scan rates the charge passed per unit time is greater, hence an increase in ip, while the total amount of charge is the same.

Anodic linear sweep voltammetry (ALSV)

It has been shown that the ALSV technique is a suitable electrochemical tool[26-28] for the characterization of electrochemically obtained thin layers of metallic alloys. Under anodic polarization conditions, the distinct components of an alloy tend to dissolve at different potentials, and the distribution of voltammetric peaks is characteristic for each alloy structure. The peak currents depend on the film thickness, while their number and potentials depend only on the alloy structure.

Effect of NaOH solution concentration

The voltammograms for the electrodeposited Zn–Co–Fe alloy on steel rod substrate dissolved anodically in NaOH solution of various concentrations (0.1 M to 0.7 M) at 30.0°C and scan rate of 50 mV s^{-1} were examined and the results of the dissolved Zn–Co–Fe alloy are given in Fig. 8. Inspection of the data of the figure reveals that the anodic peak increases and their corresponding potentials shifted towards more negative values with increasing the concentration of NaOH solution. Figure 9 represents a linear relationship between log $C_{[NaOH]}$ and log i_p of the anodic peaks of the deposited Zn–Co–Fe alloy. These results could be explained in terms of increasing the solubility of the zinc component with increasing concentration of the alkaline NaOH solution.

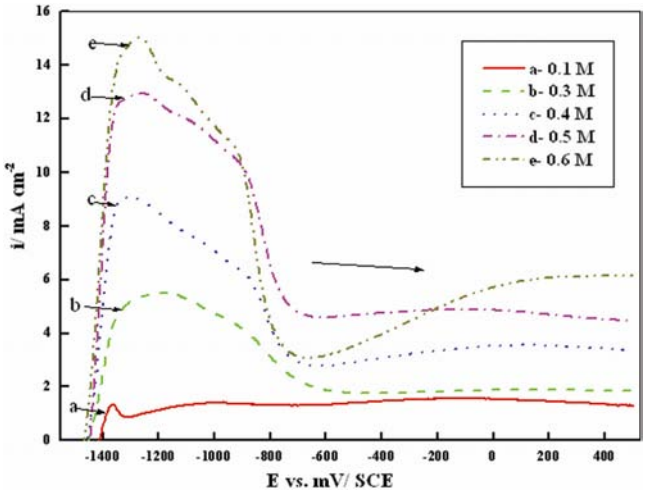

Fig. 8 — ALSV for Zn-Co-Fe alloy, electrodeposited galvanostatically on steel substrate and dissolved in different concentrations of NaOH solution at 30.0°C with scan rate 50 mV s^{-1}.

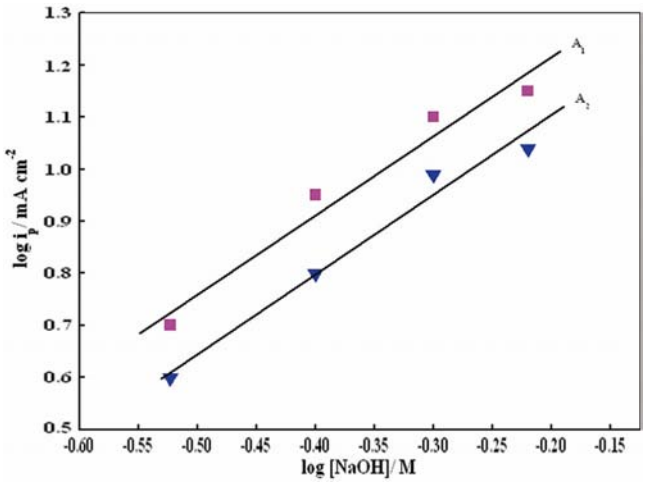

Fig. 9 — Linear dependence of the peak current density of the anodic peaks (i_p) and log [NaOH] for Zn-Co-Fe alloy, electrodeposited galvanostatically on steel substrate and dissolved in different concentrations of NaOH solution at scan rate of 50 mV s^{-1} at 30.0°C

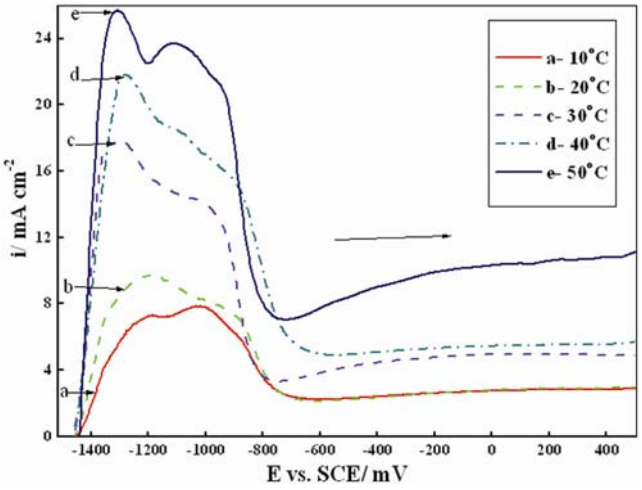

Fig. 10 — ALSV of Zn-Co-Fe alloy, electrodeposited galvanostatically on steel substrate and dissolved in 0.5 M NaOH solution with scan rate 50 mV s^{-1} at different temperature values.

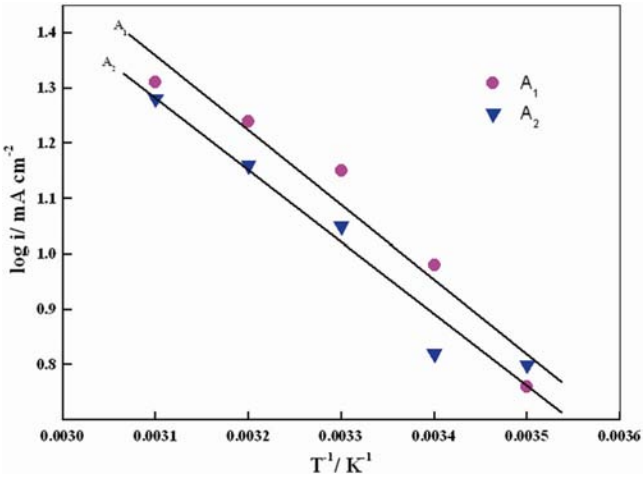

Fig. 11 — Linear dependence of (log i_p) of the anodic peaks and (1/T) for Zn-Co-Fe alloy, electrodeposited galvanostatically on steel substrate and dissolved in 0.5 M NaOH solution with scan rate 50 mV s^{-1} and at different temperature values.

Effect of NaOH solution temperature

The influence of increasing NaOH solution temperature from 10°C to 50°C on the behaviour of the electrodeposited Zn–Co–Fe alloy at a scan rate of 50 mV s^{-1} is shown in Fig. 10. The general shape of the dissolution voltammograms doesn't change by increasing the temperature. Figure 11 represents the dependence of log i_p of the anodic peaks (A_1 and A_2) and 1/T K^{-1} for electrodeposited Zn–Co–Fe alloy. The rise of solution temperature enhances the heights of the anodic peaks, and shifts the peak potentials toward more negative values. This indicates that the increase in temperature accelerates the diffusion rate of the diffusing species to or from the anode surface. Also the height of the anodic peaks i_p can be corresponded to increasing the solubility of zinc components in the deposit.

The energy of activation of the process for A_1 and A_2 from Fig. 11 were 26 and 25 kJ/mol respectively, and therefore the diffusive character of the process was confirmed.

Conclusion

From the electrochemical tests studied for the dissolution of the electrodeposited Zn-Co-Fe alloy in sodium hydroxide solution, it can be concluded that:

- The galvanostatic studies show that Zn–Co–Fe alloy offers a good corrosion resistance in comparison with zinc alone, Zn–Co and Zn–Fe binary alloys.
- SEM of the electrodeposited Zn–Co–Fe alloy show complete coating, compact and homogeneous deposits on the substrate surface. XRD showed that Zn–Co–Fe deposits consisted of a zinc solid solution, and iron–cobalt intermetallic phase (FeCo).
- The cyclic voltammograms of the electrodeposited Zn–Co–Fe alloy in NaOH solution gave two anodic dissolution peaks, the first anodic peak represents the dissolution of Zn from pure zinc phase and the second one has a complete homogeneous resulted in FeCo phase which behaves like one metal.
- Increasing scan rate increases the height of the anodic peak current density (i_p) and shifts potentials to the more noble values due to the selective dissolution of zinc increases.
- Increasing NaOH concentration and temperature enhance the height of the anodic peak current density (i_p) and shift the potentials towards more negative values attributed to increasing the solubility of the zinc component .

References

1 Tsuru T, Kobayashi S, Akiyama T, Fukushima H, Gogia S K & Kammel R, *J Appl Electrochem*, 27 (1997) 209.

2 Tomachuk C R, Freire C M A, Ballester M, Fratesi R & Roventi G, *J Surf Coat Technol*, 122 (1999) 6.

3 Abou-krisha M M & Abushoffa A M, *Int J Electrochem Sci*, 2 (2007) 418.

4 Fei J Y & Wilcox G D, *J Electrochim Acta*, 50 (2005) 2693.

5 Chen P Y & Sun I W, *J Electrochim Acta*, 46 (2001) 1169.

6 Rashwan S M, Mohamed A E, Abd El-Wahaab S M & Kamel M M, *J Appl Electrochem*, 33 (2003) 1035.

7 Neto P D L, Correia A N, Colares R P & Araujo W S, *J Braz Chem Soc*, 18 (2007) 1164.

8 Zhang Z, Leng W H, Shao H B, Zhang J Q, Wang J M & Cao C N, *J Electroanal Chem*, 516 (2001) 127.
9 Park H & Szpunar J A, *J Corros Sci*, 40 (1998) 525
10 Huang J F & Sun I W, *J Electrchem Soc*, 151 (2004) C8.
11 Bajat J B, Miskovic-Stankovic V B & Kacarevic-Popovic Z, *J Prog Org Coat*, 47 (2003) 49.
12 Ebadi M, Basirun W J, Alias Y, Mahmoudian M R & S Y Leng, *Mater Charact*, 66 (2012) 46.
13 Lodhi Z F, Mol J M C, Hovestad A, Terryn H A & De wit J H W, *J Surf Coat Technol*, 202 (2007) 84.
14 Conceicao M D, Eduardo N C & Roberto Z N, *J Mat Sci Appl*, 3 (2012) 348.
15 Abou-Krisha M M, *J Appl Surf Sci*, 252 (2005) 1035.
16 Fàbio R B, Lucia H M, *J Surf Coal Technol*, 201 (2006) 1752.
17 Afshar A, Dolati A G & Ghorbani M, *J Mater Chem & Phys*, 77 (2002) 352.
18 Jović V D, Zejnilović R M, Despić A R & Stevanović J S, *J Appl Electrochem*, 18 (1988) 511.
19 Zhang Y & Ivey D G, *J Mat Sci & Engine*, B 140 (2007) 15.
20 Abou-Krisha M M, Rageh H M & Matter E A, *J Surf Coat Technol*, 202 (2008) 3739.
21 Mckubre M C H & Macdonald D D, *J Electrochem Soc*, 128 (1981) 524.
22 Kannangara D C W & Conway B E, *J Electrochem Soc*, 134 (1987) 894.
23 Correia A N & Machado S A S, *J Appl Electrochem*, 33 (2003) 367.
24 Barbosa L L, Brito G A O, Lopez M C, Broggi R L & Carlos I A, *J Electrochem Acta*, 50 (2005) 4710.
25 Ortiz-Aparicio J L, Meas Y, Trejo G, Ortega R, Chapman T W, Chainet E & Ozil P, *J Appl Electrochem*, 41 (2011) 669.
26 Gomez E, Alcobe X & Valles E, *J Electroanal Chem*, 505 (2001) 54.
27 Jovic V D, Despic A R, Stevanovic J S & Spaic S, *J Electrochim Acta*, 34 (1989) 1093.
28 Swathirajan S, *J Electrochem Soc*, 133 (1986) 671.